REPORT, 25.08.2023

Reporting on entry project for TReNDS center: analysis of dynamic complexity (entropy) in time-windowed dynamic functional network connectivity (dFNC). Study compares dFNC of healthy controls with dFNC of schizophrenia patients.

INTRODUCTION

Functional network connectivity (FNC)

The functional network connectivity, or FNC, can be understood as the statistical dependence between the time series of separate functional networks in the human brain. A special emphasis must be placed on the word networks in this definition. Functional connectivity has, for much of its history, replied upon anatomical atlases to parcellate the brain into regions of interest (ROIs) and reported the statistical dependencies between these ROIs. The present report instead uses spatial independent component analysis (sICA) to detect spatial maps of areas which co-activate but do not overlap. This allows the authors to identify areas of interest based on functional relations rather than strictly anatomical landmarks. These functionally coherent maps constitute the functional networks, or FNs. Detection of the FNC simply requires correlating the time courses of all FNs against one another.

Dynamic Functional network connectivity (dFNC)

The functional network connectivity (FNC) is also often called the *static* functional network connectivity (sFNC) as it reports only a single value for interregional correlation over the entire length of the scan. This metric inherently assumes that interregional correlation does not change with time. Results from EEG studies have long demonstrated that this is not the case, and that interregional coupling instead varies on the order of milliseconds across the cortex. Efforts to capture this coupling in fMRI have led to, among other methods, the sliding-window approach. This method, like sFNC, measures functional coupling via Pearson correlation; however, rather than evaluating this correlation across the entire scan, it evaluates only a

section of the timeseries at a time. This allows researchers to evaluate the dynamics of interregional coupling, which has provided valuable insight into the mechanisms behind both healthy and disordered brain activity.

Shannon Entropy

The Shannon entropy is ubiquitous in signal analysis and communication studies. In this context, it is used as a measure of the amount of information that a given signal transmits over time. This is not its only use, however, as a virtually identical measure is used in statistical physics to quantify the reversibility of a system's change in state. Within statistical physics, a change in state which produces no entropy can be perfectly reversed with no net loss of energy. Any change which does produce entropy, however, cannot be reversed without an input from outside the system. In this sense, entropy is frequently used to estimate the efficiency of a physical reaction, such as the combustion which occurs inside of an internal combustion engine. Some researchers have also proposed its use to quantify the so-called "arrow of time", i.e. the irreversibility of a temporal sequence of events, as a measure of the amount of processing which a signal undergoes (de la Fuente et al. 2022; Soler-Toscano et al. 2022).

Despite its ubiquity, the entropy is a difficult thing to conceptualize. While related to certain physical variables, such as pressure and temperature, it directly corresponds to none of them. Its rather unintuitive mathematical definition,

$$S = -k_B \sum_i P_i \ln P_i$$

does not help matters much. This can make interpreting results from entropy analyses rather difficult, as it is hard to determine what alterations in a signal's properties may cause a change in measured entropy. It is perhaps this uninterpretability which led John von Neumann to tell Claude Shannon, "You should call it entropy for two reasons. First, your uncertainty function has been used in statistical mechanics under that name, so it already has a name. Second, and much more importantly, no one really knows what the entropy actually is, so in a debate you will always have the advantage."

Amusing as this anecdote is, it does point to a very real problem in the field of both statistical mechanics and information theory. A considerable portion of my Ph.D. thesis is devoted to the problem of how to interpret entropy alterations in time-series signals. To brutally summarize, it is my belief that, in the context of information theory, entropy can be best understood as an inverse measure of the predictability of a system's dynamics given known constraints. A system with highly regular, predictable dynamics will generally have lower entropy than a system with irregular, unpredictable ones. This is the definition which will be maintained for the remainder of this report.

METHODS

Dynamic Functional Network Connectivity (dFNC)

The author received a dataset which had already been segmented into functional networks (FNs) and which had already estimated the dynamic functional connectivity of those networks (dFNC) using a tapered sliding-window method. A full description of the data collection and dFNC estimation may be found in (Du et al. 2020).

Isolation of Temporal Components in dFNC

This analysis estimates the Shannon entropy of temporally independent co-activation patterns of inter-network connections (FCs). This approach has been validated in both the neural spike train (Lopes-dos-Santos et al. 2011; Lopes-dos-Santos, Ribeiro, and Tort 2013) and fMRI contexts (Deco, Cruzat Grand, and Kringelbach 2019), and is a theoretically coherent method for finding recurrent functional communities. This requires identifying spatial networks with statistically independent time courses, for which temporal independent component analysis (tICA) is the obvious tool. ICA, however, requires the number of independent components in the data, which is seldom available *a priori*. I employ the Marčenko-Pastur distribution (Blair et al. 2022) to this end, as it is both a computationally efficient and theoretically sound means of estimating the number of independent components in matrix. Once this process was

completed, I used the fastICA algorithm (Hyvärinen and Oja 2000) to isolate these components and their time courses from the space-time data matrix.

Estimation of the Entropy

Entropy is estimated at the subject level for all subjects in this dataset. Two levels of entropy estimates are employed. First, the entropy of each tICA components' time course is estimated using a variation of the Kozachenko-Leonenko entropy estimator (Singh et al. 2003; Delattre and Fournier 2017; Kozachenko and Leonenko 1987). Once the entropy of each individual component has been estimated, the joint entropy of each subject was calculated according to

$$H(C_1, \ldots, C_N) = \sum_{j=1}^{N} H(C_j)$$

It must be emphasized that this formulation of $H(C_1, \ldots, C_N)$ requires that each component's time course be statistically independent from all others (Cover and Thomas 2006). If the constituent time courses display statistical dependencies, these dependencies must be accounted for. Hence, the decision to utilize tICA is based not only on the desire to find functionally relevant communities, but also on the analytical need for independence.

Significance Tests

Group comparisons in this report primarily use the two-sided Kolmogorov-Smirnov test to determines statistical significance. A permutation-based difference-of-means test (Krol 2021) is occasionally also used, as is Student's two-sample *t*-test. Unless otherwise noted, all results should be assumed to use the Kolmogorov-Smirnov test. Multiple-comparison correction was implemented via the false discovery rate (Benjamini and Hochberg 1995). All tests used Mathwork's MATLAB version R2021a.

RESULTS

Static Functional Network Connectivity

Static functional network connectivity (sFNC) was primarily used as a sanity check to ensure that the data were not compromised before beginning the analysis. Calculation was straightforward, with the results displayed in Figure 1. Healthy controls generally display both more structured and higher-magnitude interregional correlation, something broadly supported in the neuroimaging literature.

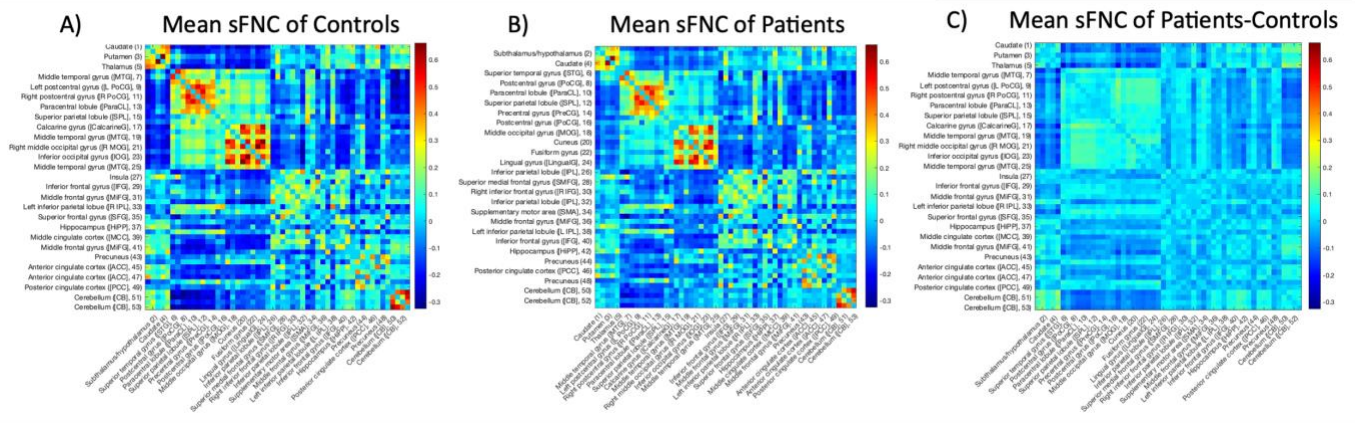

Figure 1. Static functional network connectivity (sFNC) analysis was mainly conducted as a sanity check to ensure that the received data were indeed the same as that reported in Du *et. al*. 2020 and that the author had reconstituted the matrices correctly. Panel (A) displays the average sFNC of controls in the selected dataset, while panel (B) displays the average sFNC of schizophrenia patients. A visual inspection demonstrates that both (A) and (B) display the block structure characteristic of sFNC matrices common in the functional imaging literature. As in Du *et. al*. reported this structure, it appears that the FNC matrices have indeed been correctly reconstructed.

The author observed that controls seem to display a larger range of correlation coefficient values, with higher magnitudes for both positive and negative values. To examine this, he subtracted the patient average sFNC matrix from the control average matrix. A visual examination of the resulting connectivity difference matrix does indeed suggest higher magnitude correlation coefficient values in the control population, particularly between negatively correlated areas. This reduced oppositional coupling may be relevant for future schizophrenia studies. The author suggests searching for population-level differences in subject sFNCs using the network-based statistic or other network-specific difference tests.

Dynamic Functional Network Connectivity

The data was provided to the author already processed into 137 time points, each of which contained correlation matrices calculated using a tapered sliding window (Du et al. 2020). The author could thus move directly to the estimation of the number of independent temporal components extant within the provided data. Application of the Marčenko-Pasteur theorem reliably detects 171 independent temporal components (tICs) within the vectorized connectivity data. fastICA is then applied to the 137×1378 array to isolate these 171 tICs and their time courses. The 171 53×53 spatial maps of each component are reconstructed from the 1378×171 fastICA output.

Joint Entropy

The temporal statistical independence enforced by the fastICA algorithm allows each IC's Shannon entropy to be calculated independently of the others. As the formal definition of the Shannon entropy requires knowledge of the data's complete probability distribution, which is seldom available for real datasets, researchers generally must estimate the Shannon entropy of any given time series. We opt to use a variation on the Kozachenko-Leonenko estimator (Kozachenko and Leonenko 1987; Delattre and Fournier 2017) based on *k*-nearest-neighbor distances between sample points (Singh et al. 2003; Goria et al. 2005). Running this estimation algorithm on each subject's IC time courses produces a $D \times S$ array of entropy values for patients and controls, where D is the number of ICs (171) and S the number of subjects (311). To compute subject-level joint entropy, we took the sum of this matrix along its first dimension to produce a $1 \times S$ array of joint entropy values. The Kolmogorov-Smirnov two-sample test showed that patient and subject joint entropy values differ (Figure 2), with patients displaying a small but statistically significant elevation compared to controls ($p = 7.92 \times 10^{-6}$) (Table 1). A two-sample *t*-test and a difference-of-means permutation test (Krol 2021) qualitatively confirmed this result.

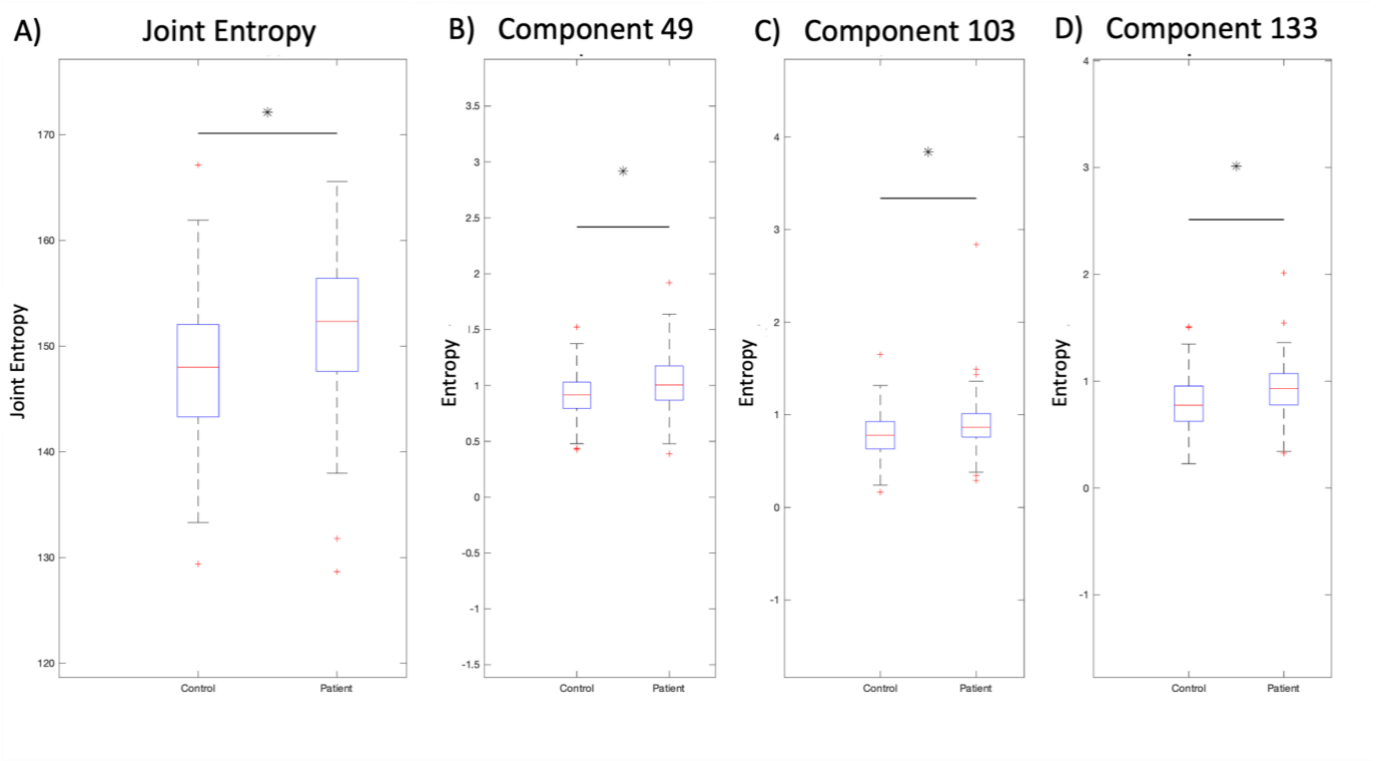

Figure 2. Upon estimating the entropy of all subjects' temporally independent components, a Kolmogorov-Smirnov two-sample test demonstrates that schizophrenia patients tend to display significantly higher entropy than the control group (A). These differences are not evenly spread throughout all components; instead, three components display statistically significant entropy elevations in the patient population (B, C, D). It thus appears that schizophrenia affects specific components (meta-states, if you will) of the human brain's functional connectivity, which may offer a path for further investigation and treatment.

	Mean	Standard Deviation
Controls	147.43	6.86
Patient	151.93	6.45

Table 1 displays the mean and standard deviations of the joint entropy of both control and patient populations. While the majority of each distribution falls within the other's standard deviation, they remain sufficiently separated to be distinguishable. Patients generally display higher joint entropy, a theme which is consistent with previous work using the LEICA and tICA methods.

Component Entropy

We considered it probable that group-level entropy alterations concentrate in specific ICs rather than being evenly distributed across all datasets. With this in mind, we elected to compare the group-specific entropies of each IC, again primarily using the Kolmogorov-Smirnov two-sample test. Multiple comparison correction utilized the false discovery rate (Benjamini and Hochberg 1995). The Jarque-Bera test suggested that component-level subject entropies do not follow a normal distribution, so the *t*-test was dispensed with.

A total of three (3) components display sufficiently elevated group-level entropy in patients to survive family-wise error correction (false discovery rate, or FDR). Means and standard deviations may be viewed in Table 2 and Figure 2. Figure 3 displays the time courses and connectivity matrices of the components with altered dynamics in patients. Interestingly, the connectivity matrices display symmetry about the anti-diagonal (running from left bottom to right top corner). This may suggest an error in reconstructing the sFNC matrix, as these matrices typically display symmetry about the main diagonal. The author wishes to examine the reconstruction for possible errors. In addition, all three of the components with altered entropy display singular, very large spikes in time course readings, which may be the cause of the observed entropy differences. If this is the case, care should be taken to confirm that these spikes accurately reflect the data rather than being the result of scanning or analytical artifacts.

	Control		Patients	
	Mean	**Standard Deviation**	**Mean**	**Standard Deviation**
Component 49	0.9146	0.2020	1.0244	0.2363
Component 103	0.7817	0.2324	0.8805	0.2704
Component 133	0.7974	0.2499	0.9317	0.2319

Table 2 displays the mean and standard deviations of Shannon entropy in the three components which were found to significantly differ between populations. In all three components, patients display substantially elevated entropy compared to controls.

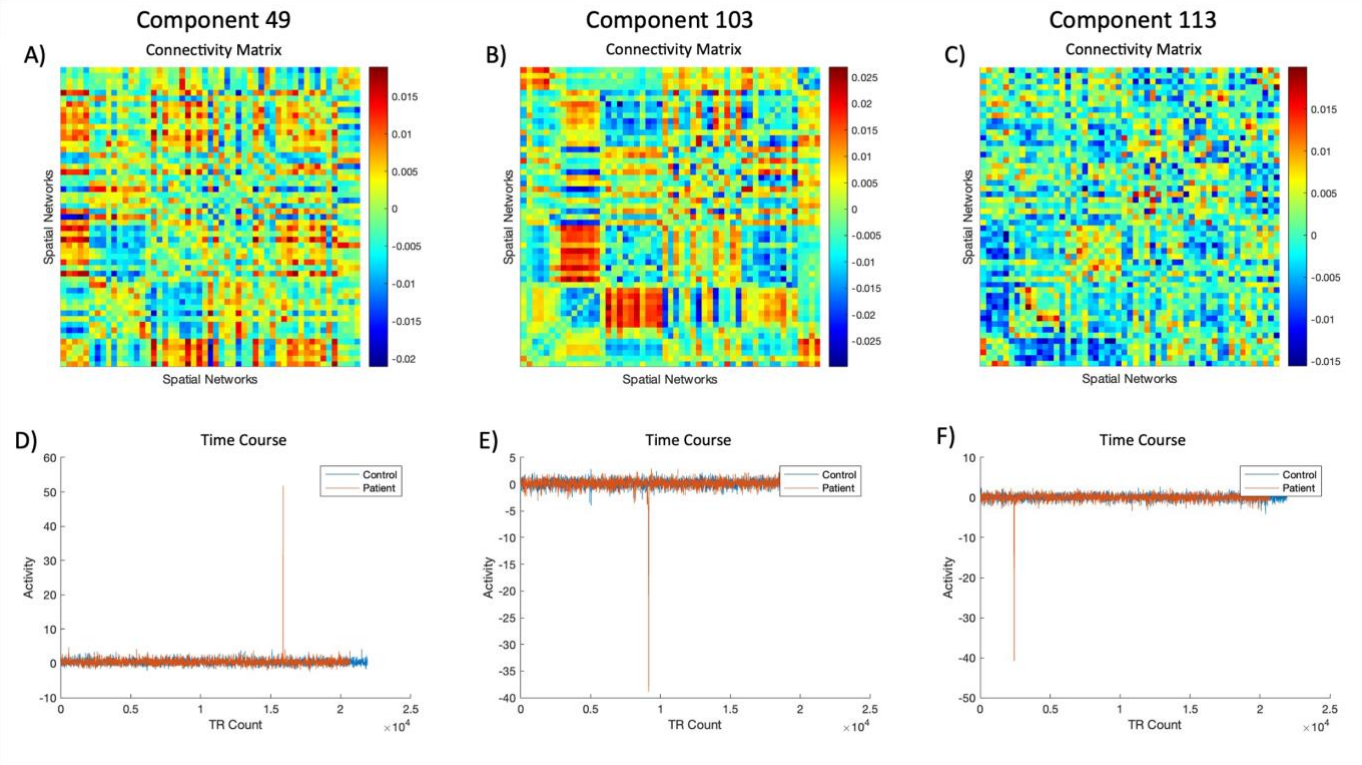

Figure 3. The connectivity matrices and time courses of the three components which display elevated entropy. Component 49 (A: connectivity matrix; D: time course) displays a weak block structure. A different block structure is evident in Component 103 (B: connectivity matrix; E: time course). Component 113, on the other hand, has very weak structure (C: connectivity matrix; F: time course) everywhere except in the bottom left corner, where a weakly anticorrelated block is visible. All three components' connectivity matrices appear to be symmetric about the anti-diagonal (running from left bottom to right top corner). This may suggest an error in reconstructing the sFNC matrix, as these matrices typically display symmetry about the main diagonal. The author wishes to examine the reconstruction for possible errors.

Entropy and Clinical Scores

Given the observed population-level changes in joint and component entropy, the next obvious question is whether these observed changes reflect known clinical or population-based variables. With this in mind, we correlated known the known clinical variables (included in the dataset) with both joint and component-level entropy distributions. Of the resulting matrix of correlation coefficients and *p*-values, 17 survive family-wise error multiple comparison correction. These 17 surviving correlation coefficients may be viewed in Table 3, along with the variables and components to which they correspond.

Variable	Component	ρ	p
Diagnosis	Joint	0.320512	0.000000
VerbalLearning	Joint	-0.220490	0.000195
VisualLearning	Joint	-0.235446	0.000076
CMINDS_composite	Joint	-0.277205	0.000004
CMINDS_composite	3	-0.222672	0.000220
AttentionVigilance	44	-0.225382	0.000168
Diagnosis	49	0.243537	0.000014
SpeedOfProcessing	49	-0.213962	0.000311
CPZ	66	0.537245	0.000000
Diagnosis	99	0.202159	0.000333
SpeedOfProcessing	103	-0.234416	0.000075
WorkingMemory	103	-0.279095	0.000002
VisualLearning	103	-0.222014	0.000195
CMINDS_composite	105	-0.224234	0.000198
Diagnosis	133	0.268625	0.000002
age	148	0.274741	0.000001
VisualLearning	148	-0.213171	0.000353

Table 3 displays the correlation of joint and component entropies which survive multiple comparison correction (FDR). Unsurprisingly, joint entropy and components 49, 103, and 133 all correlate with diagnosis. This is to be expected, as all three displayed significant alterations in entropy between populations. Component 99 also appears to correlate with diagnosis, albeit to a lesser degree than these three. Joint entropy proved the single most predictive physiological reading, covering four of the fourteen clinical variables examined. Of note, only nine of the fourteen clinical variables appear in this table; gender, PANSS scores (positive and negative), reasoning and problem-solving, and scanning site appear to have no effect on entropy at the group level. This is somewhat surprising, as PANSS is specifically intended to detect schizophrenia and thus should correlate with any variable related to schizophrenia. Most likely, this simply reflects the fact that PANSS scores were not reported for the control group. Nonetheless, it may be worth evaluating the degree to which PANSS predicts dynamic functional metrics in a separate study. It is also noteworthy that reasoning and problem-solving scores appear unrelated to entropy despite some literature suggesting that it is affected in schizophrenia. Apparently this association is not strong enough to correlate with entropy, which suggests that it may be poorly related to schizophrenia diagnosis as well.

Joint entropy proved the single most predictive reading, covering four of the fourteen clinical variables examined. Of note, only nine of the fourteen clinical variables appear in this table; gender, PANSS scores (positive and negative), reasoning and problem-solving, and scanning site appear unaffected by entropy at the group level. This is somewhat surprising, as PANSS is specifically intended to detect schizophrenia and thus should correlate with any variable related to schizophrenia. Most likely, this simply reflects the fact that PANSS scores were not reported for the control group. Nonetheless, it may be worth evaluating the degree to which PANSS predicts dynamic functional metrics in a separate study. It is also noteworthy that reasoning and

problem-solving scores appear unrelated to entropy despite some literature suggesting that it is affected in schizophrenia. Apparently, this association is not strong enough to correlate with entropy, which suggests that it may be poorly related to schizophrenia diagnosis as well. Of the observed clinical variables, CMINDS composite scores, processing speed, and visual learning are the most associated with specific component entropies. Visual learning and CMINDS scores also associate with joint entropy scores. Other clinical variables appear to be associated with specific tICs, suggesting a degree of specificity in these components' function and activity. Notably, most relations are negative, implying that increased entropy leads to lower clinical test scores. The only exceptions (aside from diagnostic status) are CPZ scores (tIC 99) and age (tIC 148).

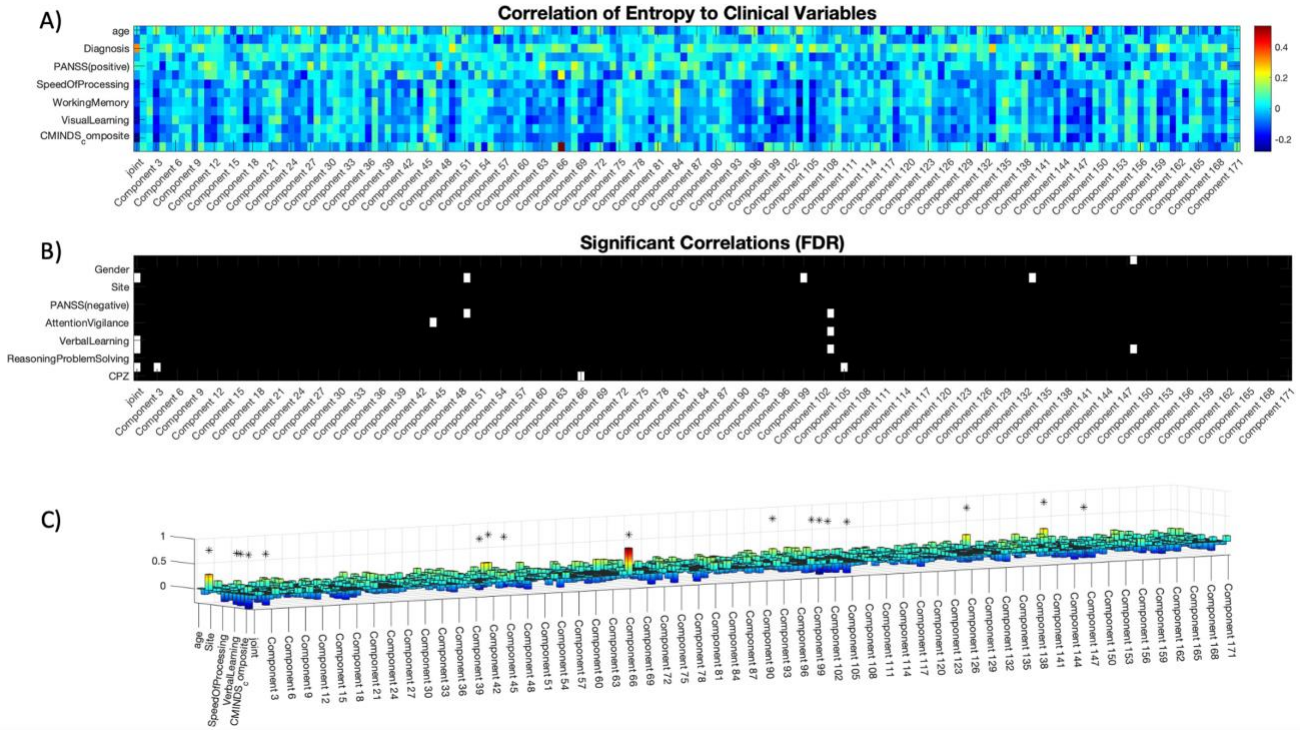

Figure 4. A correlation of tIC entropy scores with the fourteen clinical variables in this dataset (A) reveals that nine clinical variables significantly correlate with joint or component-level entropy (B). Four tICs appear to relate to diagnostic status. Although tIC 99 does not survive multiple-comparison correction, it may merit further examination. Oddly, tIC 99 does not correspond to any other clinical variable, appearing only in the diagnostic row. By contrast, other diagnostic-sensitive tICs predict one or more clinical variables. Most often, these are negatively related, which suggests that patients score lower on the relevant clinical tests than controls do. Two notable exceptions exist: tIC 66 positively predicts CPZ scores, and tIC 148 positively predicts age. Nonetheless, the trend towards negative associations is far broader (C).

DISCUSSION

Static Functional Network Connectivity

Previous work on this dataset (Du et al. 2020) established that grand average (static) functional network connectivity (sFNC) demonstrated diminished connectivity between cerebellum and thalamus, caudate, and subthalamus. On the other hand, links from thalamus and caudate to postcentral gyrus and superior temporal gyrus, and from subthalamus to superior temporal gyrus, demonstrated increased functional connectivity over the course of the scan. The author intends to run a network-based statistic analysis of subject-level sFNC to determine whether a similar pattern holds in his analysis, as this would further validate his reconstruction methods.

Dynamic Functional Network Connectivity

Joint Entropy

The finding of increased joint entropy in patients at first appears somewhat surprising. Multiple studies [citation needed] note that schizophrenia appears to be characterized by both reduced overall functional connectivity (Du et al. 2020) and reduced functional connectivity dynamism (Miller et al. 2016). These findings suggest that schizophrenia patients should display *decreased* entropy in their dFNC signals, yet we find the opposite even (with one exception) at the level of individual temporal independent components (tICs).

One should recall, however, that entropy does not only quantify the range of values which a signal may take, but also the predictability of those values and their interdependencies. In other words, if observing signal *A* at time *t* provides information on *A* at *t+1*, but the same observation on *A'* provides no information on *A'* at *t+1*, then signal *A* will have lower entropy than signal *A'*. The increased entropy of schizophrenia dFNC dynamics may therefore indicate that schizophrenia reduces the predictability of transitions between connectivity states. Prior work

has demonstrated that healthy controls display relatively predictable co-activation state dynamics (Betzel et al. 2016; Gu et al. 2018; 2017; Ashourvan et al. 2021), i.e. knowing the brain's current functional connectivity map allows one to predict the following one with high accuracy. The present results suggest that such transitions may become less structured in schizophrenia, i.e. a flattened probability distribution of future states. The connectivity dysfunction known to exist in schizophrenia and bipolar disorder may reflect this.

Component Entropy

The dFNC dynamics of individual tICs are not as well documented as those of the whole brain. I am, in fact, not aware of any study which has directly compared the time courses of individual tICs in schizophrenia patients to their equivalents in healthy controls. As such, I have little context in which to explore the reported results of this analysis. In broad terms, however, the conclusions of the previous section hold: increased entropy in schizophrenia patients suggest less predictable activity dynamics. Although previous work suggests that schizophrenia patients operate within a smaller space of dFNC states, these results suggest that their movement within that space has been randomized to a much higher degree than healthy persons'. The opposite, of course, holds for the single tIC which displays higher entropy in controls than in patients. The unexplained spikes in the time courses of the highlighted tICs, however, must be borne in mind. Until these results have been confirmed, strong conclusions should be avoided.

Entropy and Clinical Scores

The association of specific tICs with specific clinical variables suggests a level of specificity in the functional roles of these tICs. It may be worth probing the links between these behavioral and neuroimaging features further. Of the nine clinical variables found to associate with entropy scores, five (verbal learning, attention and vigilance, working memory, and age) appear affected by individual tICs, with multiple tICs splitting responsibility for the other four. It would be interesting to see whether these tICs, or some linear combination thereof, correspond to functional networks known to control these clinical variables.

Caveats

The primary caveat of this article is that the number of tICs displaying statistically significant populations differences in entropy appears to vary between runs. This is strange, as the author believes that the fastICA algorithm is largely deterministic and so should provide similar results over multiple runs. A more precise entropy estimation algorithm may be needed. A stricter multiple comparison correction method may also stabilize the number of tICs which survive.

CONCLUSION

Overall, it appears that spatiotemporal independent component entropy can predict the diagnosis of schizophrenia at both joint and component level. Initial results suggest that individual tICs contribute to specific behavioral and cognitive deficits in schizophrenia patients, which raises the possibility of treatment which could target these specific traits. These results also point to the possibility of classifying patients according to cognitive-behavioral scores. This may, in the long term, prove a more flexible and valuable means to prescribe treatments than the strictly categorical framework of the DSM-V and ICD, as these categorical diagnoses are known to correlate poorly with treatment outcomes. In addition, if cognitive-behavioral dimensions correspond to particular functional systems, charting a patient's position in such a space may allow more precise treatment than current methods permit. The author hopes to assist in the movement towards such a framework.

BIBLIOGRAPHY

Ashourvan, Arian, Preya Shah, Adam Pines, Shi Gu, Christopher W. Lynn, Danielle S. Bassett, Kathryn A. Davis, and Brian Litt. 2021. “Pairwise Maximum Entropy Model Explains the Role of White Matter Structure in Shaping Emergent Co-Activation States.” *Communications Biology* 4 (1). https://doi.org/10.1038/s42003-021-01700-6.

Benjamini, Yoav, and Yosef Hochberg. 1995. “Controlling the False Discovery Rate : A Practical and Powerful Approach to Multiple Testing.” *Journal of the Royal Statistical Society. Series B (Methodological).* 57 (1): 289–300.

Betzel, Richard F., Shi Gu, John D. Medaglia, Fabio Pasqualetti, and Danielle S. Bassett. 2016. “Optimally Controlling the Human Connectome: The Role of Network Topology.” *Scientific Reports* 6 (1): 30770. https://doi.org/10.1038/srep30770.

Blair, David Sutherland, Carles Soriano-Mas, Joana R. B. Cabral, Pedro Moreira, Pedro Morgado, and Gustavo Deco. 2022. “Complexity Changes in Functional State Dynamics Suggest Focal Connectivity Reductions.” *Frontiers in Human Neuroscience* 16 (September): 1–18. https://doi.org/10.3389/fnhum.2022.958706.

Cover, Thomas M., and Joy A. Thomas. 2006. *Elements of Information Theory*. *Elements of Information Theory*. Second Edi. Hoboken, New Jersey: John Wiley & Sons, Ltd. https://doi.org/10.1002/047174882X.

Deco, Gustavo, Josefina Cruzat Grand, and Morten L. Kringelbach. 2019. “Brain Songs Framework Used for Discovering the Relevant Timescale of the Human Brain.” *Nature Communications* 10 (1): 1–13. https://doi.org/10.1038/s41467-018-08186-7.

Delattre, Sylvain, and Nicolas Fournier. 2017. “On the Kozachenko–Leonenko Entropy Estimator.” *Journal of Statistical Planning and Inference* 185 (June): 69–93. https://doi.org/10.1016/j.jspi.2017.01.004.

Du, Yuhui, Zening Fu, Jing Sui, Shuang Gao, Ying Xing, Dongdong Lin, Mustafa Salman, Anees Abrol, Md Abdur Rahaman, Jiayu Chen, L. Elliot Hong, Peter Kochunov, Elizabeth A. Osuch, and Vince D. Calhoun. 2020. “NeuroMark: An Automated and Adaptive ICA Based Pipeline to Identify Reproducible FMRI Markers of Brain Disorders.” *NeuroImage: Clinical* 28 (January): 102375. https://doi.org/10.1016/j.nicl.2020.102375.

Goria, M. N., N. N. Leonenko, V. V. Mergel, and P. L. Novi Inverardi. 2005. “A New Class of Random Vector Entropy Estimators and Its Applications in Testing Statistical Hypotheses.” *Journal of Nonparametric Statistics* 17 (3): 277–97. https://doi.org/10.1080/10485250410002681 5.

Gu, Shi, Richard F. Betzel, Marcelo G. Mattar, Matthew Cieslak, Philip R. Delio, Scott T. Grafton, Fabio Pasqualetti, and Danielle S. Bassett. 2017. “Optimal Trajectories of Brain State Transitions.” *NeuroImage* 148 (March): 305–17. https://doi.org/10.1016/j.neuroimage.2017.01.003.

Gu, Shi, Matthew Cieslak, Benjamin Baird, Sarah Feldt Muldoon, Scott T. Grafton, Fabio Pasqualetti, and Danielle S. Bassett. 2018. “The Energy Landscape of Neurophysiological Activity Implicit in Brain Network Structure.” *Scientific Reports* 8 (1): 2507. https://doi.org/10.1038/s41598-018-20123-8.

Hyvärinen, Aapo, and Erkki Oja. 2000. “Independent Component Analysis: Algorithms and Applications.” *Neural Networks*. Vol. 13. https://doi.org/10.1016/S0893-6080(00)00026-5.

Kozachenko, L. F., and N. N. Leonenko. 1987. “SAMPLE ESTIMATE OF THE ENTROPY OF A RANDOM VECTOR.” *Problems of Information Transmission*.

Krol, Laurens R. 2021. “Permutation Test.” Berlin: GitHub. https://github.com/lrkrol/permutationTest.

la Fuente, Laura Alethia de, Federico Zamberlan, Hernán Bocaccio, Morten L. Kringelbach, Gustavo Deco, Yonatan Sanz Perl, Carla Pallavicini, and Enzo Tagliazucchi. 2022.

"Temporal Irreversibility of Neural Dynamics as a Signature of Consciousness." *Cerebral Cortex*, 1–10. https://doi.org/10.1093/cercor/bhac177.

Lopes-dos-Santos, Vítor, Sergio Conde-Ocazionez, Miguel A.L. Nicolelis, Sidarta T. Ribeiro, and Adriano B.L. Tort. 2011. "Neuronal Assembly Detection and Cell Membership Specification by Principal Component Analysis." *PLoS ONE* 6 (6). https://doi.org/10.1371/journal.pone.0020996.

Lopes-dos-Santos, Vítor, Sidarta T. Ribeiro, and Adriano B.L. Tort. 2013. "Detecting Cell Assemblies in Large Neuronal Populations." *Journal of Neuroscience Methods* 220 (2): 149–66. https://doi.org/10.1016/j.jneumeth.2013.04.010.

Miller, Robyn L, Maziar Yaesoubi, Jessica A Turner, Daniel Mathalon, Adrian Preda, Godfrey Pearlson, Tulay Adali, and Vince D. Calhoun. 2016. "Higher Dimensional Meta-State Analysis Reveals Reduced Resting FMRI Connectivity Dynamism in Schizophrenia Patients." *PLoS ONE* 11 (3): 149849. https://doi.org/10.1371/journal.pone.0149849.

Singh, Harshinder, Neeraj Misra, Vladimir Hnizdo, Adam Fedorowicz, and Eugene Demchuk. 2003. "Nearest Neighbor Estimates of Entropy." *American Journal of Mathematical and Management Sciences* 23 (3–4): 301–21. https://doi.org/10.1080/01966324.2003.10737616.

Soler-Toscano, Fernando, Javier A. Galadí, Anira Escrichs, Yonatan Sanz Perl, Ane López-González, Jacobo D. Sitt, Jitka Annen, Olivia Gosseries, Aurore Thibaut, Rajanikant Panda, Francisco J. Esteban, Steven Laureys, Morten L. Kringelbach, José A. Langa, and Gustavo Deco. 2022. "What Lies underneath: Precise Classification of Brain States Using Time-Dependent Topological Structure of Dynamics." *PLoS Computational Biology* 18 (9): 1–20. https://doi.org/10.1371/journal.pcbi.1010412.